Magnetic properties of SA-$Fe_{2.75}Mn_{0.25}O_4$/ Ag ferrogels and its potential application as hyperthermia therapy material

Cite as: AIP Conference Proceedings **2353**, 030124 (2021); https://doi.org/10.1063/5.0052542
Published Online: 25 May 2021

Nadiya Miftachul Chusna, Sunaryono Sunaryono, Ahmad Taufiq, et al.

Magnetic Properties of SA-$Fe_{2.75}Mn_{0.25}O_4$/Ag Ferrogels and Its Potential Application as Hyperthermia Therapy Material

Nadiya Miftachul Chusna[1], Sunaryono Sunaryono[1,a], Ahmad Taufiq[1], and Nik Ahmad Nizam Nik Malek[2,3]

[1]*Department of Physics, Faculty of Mathematics and Natural Sciences, Universitas Negeri Malang, Jl. Semarang 5, Malang 65145, Indonesia*

[2]*Department of Biosciences, Faculty of Science, Universiti Teknologi Malaysia (UTM), 81310 UTM Johor, Malaysia*

[3]*Centre for Sustainable Nanomaterials (CSNano), Ibnu Sina Institute for Scientific and Industrial Research (ISI-ISIR), Universiti Teknologi Malaysia (UTM), 81310 UTM Johor, Malaysia*

[a]Corresponding author: sunaryono.fmipa@um.ac.id

Abstract. The SA-$Fe_{2.75}Mn_{0.25}O_4$/Ag ferrogel has been successfully synthesized using the encapsulsion method. The crystal structure characterization of the $Fe_{2.75}Mn_{0.25}O_4$/Ag material was carried out using the XRD instrument. The XRD data analysis showed the appearance of peaks of the Fe_3O_4 phase and the Ag phase in the sample diffraction pattern. Furthermore, the characterization of the functional group SA-$Fe_{2.75}Mn_{0.25}O_4$/Ag was conducted using the FTIR instrument which the results showed that the resulting functional group bonds correspond to the wavelength range of the constituent atoms. The magnetic properties of the SA-$Fe_{2.75}Mn_{0.25}O_4$/Ag ferrogel were characterized using a VSM instrument. This characterization resulted in a hysteresis curve indicating that the magnetic properties of the SA-$Fe_{2.75}Mn_{0.25}O_4$/Ag ferrogel behavior as superparamagnetic. Its potential application as a material in hyperthermia therapy is characterized by using a series of magnetic induction devices that produce optimal SAR (Specific Absorption Rate) values. The SAR values of ferrogel SA-$Fe_{2.75}Mn_{0.25}O_4$/Ag at a frequency of 483 and 553 Hz were 0.12 and 0.24 W/g, respectively.

INTRODUCTION

Ferrogel is a very sensitive material [1] and elastic [2] when given an external magnetic field. Ferrogel consists of a magnetite nano particle composite material and a polymer hyrodel matrix [3]. This material has been widely applied in the biomedical field such as magnetic resonance imaging (MRI), drug delivery [4], antifungal agent [5], anti-toxic agent [6], antibacterial agent [7], hyperthermia therapy [8], and other applications. Some of the ferrogels that were successfully reported by previous researchers were generally ferrogels with polymer-based matrix CMC [9], PVA [10] and PVP [11]. There are also studies using sodium alginate (SA) polymers in synthesizing ferrogel for application in the biomedical field [12–16]. This choice is motivated by one of the advantages of SA polymers which are biodegradable [17].

In hyperthermia therapy applications, the ferrogel is given an external magnetic field generated by an electromagnetic coil energized by AC [18]. Through the influence of the external magnetic field, the magnetic filler scattered in the ferrogel will experience an increase in spin magnetic interactions and cause an increase in temperature on the ferrogel. Increasing the temperature of the ferrogel will have an impact on increasing the SAR value which can be analyzed and used for hyperthermia therapy. Thus, the selection of magnetic and matric polymer fillers is important in ferrogel fabrication.

Matteo volio *et al*. succeeded in synthesizing Fe_3O_4 nanoparticles with a size of about 10 - 18 nm and successfully characterized the magneto-thermal particles of Fe_3O_4 with different SAR values when put into solution (67 W/g) and gel (25 W/g) [19]. Meanwhile, Jadhav *et al*. succeeded in fabricating $La_{0.7}Sr_{0.3}MnO_3$ (LSMO) magnetic nanoparticles with PVA and PEG coating. Through the heating induction test, the SAR value of the LSMO nanoparticle with PVA or PEG coating increased on average from ~ 21 to ~ 81 W/g and this result was considered to be higher than the SAR

International Conference on Life Sciences and Technology (ICoLiST 2020)
AIP Conf. Proc. 2353, 030124-1–030124-7; https://doi.org/10.1063/5.0052542
Published by AIP Publishing. 978-0-7354-4096-8/$30.00

value of the LSMO nanoparticle without coating [20]. In previous studies, the fabrication of the $Mn_{0.25}Fe_{2.75}O_4$/Ag nanocomposite was also successfully conducted with a SAR value of 0.19 W/g [21]. In further studies the resulting nanocomposite particles behavior superparamagnetic [22]. The characteristics of the magnetic properties of the material are what is needed in hyperthermia therapy [23]. However, it is still rare to report the fabrication of ferrogel using iron sand-based SA polymer hydrogels and its potential studies for the therapy of hyperthermia. Thus, it is important to study the characterization of the magnetic properties and SAR value of the ferrogel SA-$Fe_{2.75}Mn_{0.25}O_4$/Ag.

EXPERIMENTAL DETAILS

Synthesis of $Fe_{2.75}Mn_{0.25}O_4$/Ag

Material $Fe_{2.75}Mn_{0.25}O_4$ was successfully synthesized using the coprecipitation method. This method begins with separating natural iron sand using permanent magnets. The separated magnetic material was mixed with HCl solution (from Merck) using a magnetic stirrer hotplate at room temperature for 30 min. The stirred mixture was filtered to produce a solution of $FeCl_2$ and $FeCl_3$ and then mixed with $MnCl_2.4H_2O$ (from Merck). The solution is then titrated using NH_4OH (from Merck) to form a thick black precipitate. The precipitate was washed repeatedly using distilled water to form nano particles $Fe_{2.75}Mn_{0.25}O_4$.

The synthesis of $Fe_{2.75}Mn_{0.25}O_4$/Ag nanocomposite was successfully carried out using chemical reduction methods. $Fe_{2.75}Mn_{0.25}O_4$ nanoparticles from the previous process were sonicated using an ultrasonic bath for 10 min. Then the sample was mixed with $AgNO_3$ using a magnetic stirrer hotplate until evenly distributed. The resulting mixture is then titrated using NH_4OH to form a precipitate. The resulting precipitate was washed using methanol and distilled water to form $Fe_{2.75}Mn_{0.25}O_4$/Ag nanocomposites.

Fabrication of SA-$Fe_{2.75}Mn_{0.25}O_4$/Ag Ferrogel

The SA-$Fe_{2.75}Mn_{0.25}O_4$/Ag ferrogel has been successfully manufactured using the encapsulation method. Sodium alginate is dissolved into distilled water which has been heated at a temperature of about 75 - 85 °C. During the SA dissolving process, the distilled water temperature was maintained stable in the range 75 - 85 °C until the SA hydrogel mixture was obtained. After the SA hydrogel was completely formed, the $Fe_{2.75}Mn_{0.25}O_4$/Ag nanocomposite filler was mixed into the SA hydrogel. To speed up the process of forming SA-$Fe_{2.75}Mn_{0.25}O_4$/Ag ferrogel, a mixture of $Fe_{2.75}Mn_{0.25}O_4$/Ag nanocomposite filler and SA hydrogel matrix was immersed in CaCl solution. This process ends until the ferrogel SA-$Fe_{2.75}Mn_{0.25}O_4$/Ag is formed.

Characterization

To characterize the nanostructures, lattice parameters and crystal size of $Fe_{2.75}Mn_{0.25}O_4$/Ag nanocomposites, successful samples were characterized using the XRD (X-Ray Diffraction) instrument PANalytical, Type: E'xpert Pro carried out in the mineral and material laboratory of FMIPA UM. FTIR (Fourier Transform Infrared spectroscopy) Brand Shimadzu, Type: IRPrestige21 was successfully used to characterize the absorption of the ferrogel functional group $Fe_{2.75}Mn_{0.25}O_4$/Ag. Furthermore, VSM (Vibrating Sample Magnetometer) was used to characterize the magnetizing properties of $Fe_{2.75}Mn_{0.25}O_4$/Ag ferrogel. And the magnetic induction device was carried out to assess the thermal changes of $Fe_{2.75}Mn_{0.25}O_4$/Ag ferrogel with respect to time changes. The SAR value of ferrogel $Fe_{2.75}Mn_{0.25}O_4$/Ag can be seen from the linear gradient analysis of the relationship between thermal changes with time.

RESULTS AND DISCUSSION

X-Ray Diffraction Characterization

The X-ray Diffraction pattern of $Fe_{2.75}Mn_{0.25}O_4$/Ag nanocomposites is shown in Figure 1. Analysis of the crystal structure of $Fe_{2.75}Mn_{0.25}O_4$/Ag nanocomposites was successfully carried out using Rietica software. The data analysis process is carried out by matching the experimental data shown with a black circle and the model data marked with a red line as shown in Figure 1. Based on the data analysis, the $Fe_{2.75}Mn_{0.25}O_4$ ang Ag phase structures correspond to

the AMCSD model data 0002762 and AMCSD 0011135, respectively. The detected phase structure also agrees with the study reported by Sun *et al*. [21], Jiang *et al*. [22], Tung *et al*. [23], and other researchers [24–27]. The diffraction peaks of the $Fe_{2.75}Mn_{0.25}O_4$ phase structure were detected at 2θ angles of 30.08°, 35.44°, 42.64°, 57.01° and 62.39° with hkl (220), (311), (400), (333), and (422) plane, respectively [28–31]. While the diffraction peaks of the Ag phase structure were detected at 2θ, namely 38.07°, 44.24°, 64.56°, and 77.68° with the hkl (111), (200), (220), and (311) plane, respectively [28-30]. XRD data analysis also shows that the percentage composition of the nanocomposites consists of 75.78% in the form of $Fe_{2.75}Mn_{0.25}O_4$ phase structure while the remaining 24.22% is the phase structure of Ag.

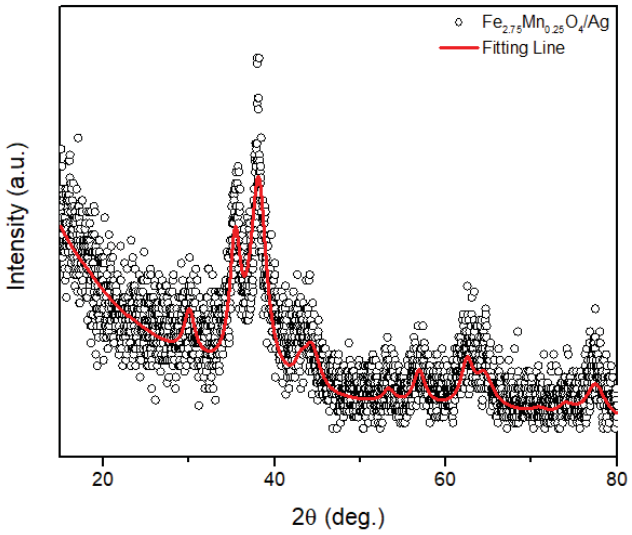

FIGURE 1. Profile of X-ray Diffraction of $Fe_{2.75}Mn_{0.25}O_4$/Ag nanocomposites

Analysis of the crystal size of $Fe_{2.75}Mn_{0.25}O_4$/Ag nanocomposites was conducted using Lorentzian modeling through the Scherrer equation approach as in Equation (1) [32].

$$\beta = K\frac{\lambda}{D\cos\theta} \quad (1)$$

β is the crystal size of the sample, k is a constant, and θ is the diffraction angle. Through Equation (1), the average crystal size of the $Fe_{2.75}Mn_{0.25}O_4$ and Ag phases is 6.57 and 9.98 nm, correspondingly. This crystal size is relatively smaller when compared to the crystal size obtained from the results of a study reported by Tung *et al*., namely 17 - 18 nm [23]. With a small crystal size, the $Fe_{2.75}Mn_{0.25}O_4$/Ag nanocomposite is ideal to be a magnetic filler as a candidate for hyperthermia therapy.

FTIR Characterization

The infrared spectrum of the SA- $Fe_{2.75}Mn_{0.25}O_4$/Ag ferrogel is presented in Figure 2. Based on the analysis of infrared spectrum data, the vibrations of the atomic bonds that make up the ferrogel occur at wave numbers 998 - 1022 and 1503 - 1515 cm^{-1}. The vibration in the wave number represents the amine group due to the pereductor in the formation of Ag [18]. Meanwhile, vibration due to the O-H group was detected in wave numbers 1634 - 1638 and 3418 - 3454 cm^{-1} [27-33]. This functional group shows the presence of H_2O bonds which are included in the SA-$Fe_{2.75}Mn_{0.25}O_4$/Ag ferrogel.

The presence of the $Fe_{2.75}Mn_{0.25}O_4$ phase structure was detected at the absorption of wave numbers 642 and 1360 cm^{-1} [34,35]. The absorption of these wave numbers is characteristic of vibrations due to the Fe-O bond. Other vibrations due to Fe-O bonds were also detected at wave numbers 417 - 510 cm^{-1} [36]. Interestingly, absorption of functional groups was also observed at wave number 521 cm^{-1}, which is vibrations due to Fe-O bonds. This Fe-O bond occupies a tetrahedral which is most likely a representation of the Mn atom [27]. Mn atoms partially replace Fe atoms as a result of the pending process [37]. In addition, functional group absorption also occurs at wave numbers 1607 and

1410 cm^{-1}. The absorption in the area is a vibration of COO- due to the presence of SA polymer [36–38]. Thus, all the atomic elements that make up the ferrogel SA-$Fe_{2.75}Mn_{0.25}O_4$/Ag can be detected properly in the infrared spectrum.

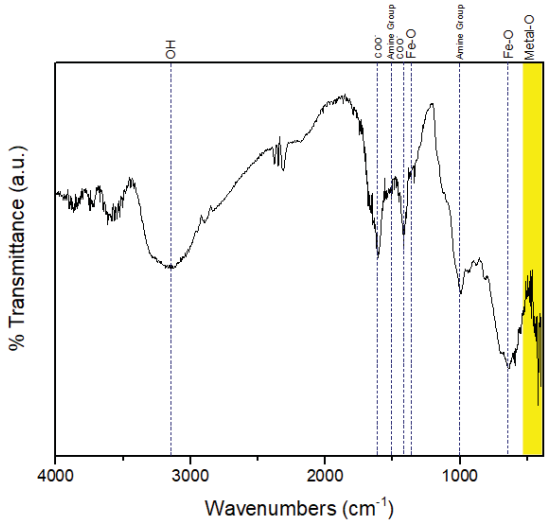

FIGURE 2. IR spectrum of SA-$Fe_{2.75}Mn_{0.25}O_4$/Ag ferrogel

Magnetic Properties

Figure 3 is the hysteresis curve of the SA- $Fe_{2.75}Mn_{0.25}O_4$/Ag ferrogel using the VSM instrument. The experimental data shown by the black circle was refined using the Langevin modeling marked with a red line. The refinement results show good accuracy between the experimental data and the model data in the form of a hysteresis curve. The ferrogel hysteresis curve produces magnets of magnetization in the form of remanent magnetization (M_r), coercivity value (H_c) and saturation magnetization (M_s).

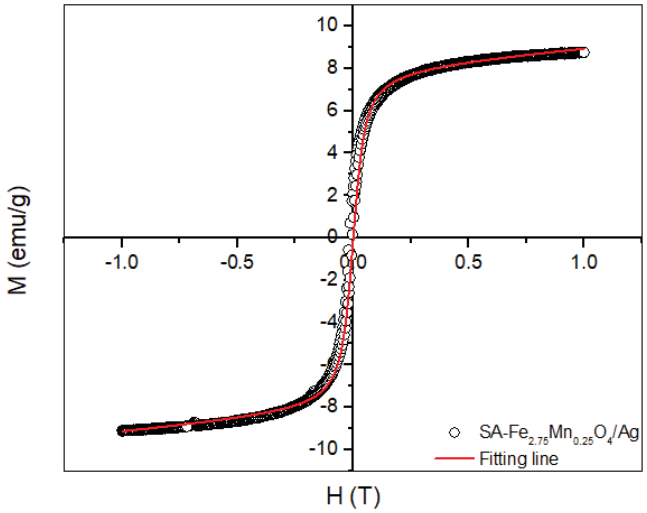

FIGURE 3. Hysteresis curve of SA-$Fe_{2.75}Mn_{0.25}O_4$/Ag ferrogel

Based on the data analysis, the remanent magnetization value, the coercivity (H_c) value and the saturation magnetization value of the SA- $Fe_{2.75}Mn_{0.25}O_4$/Ag ferrogel were 0.094 emu/g, 0.023 T, and 8.19 emu/g, respectively. The SA-$Fe_{2.75}Mn_{0.25}O_4$/Ag ferrogel coercivity field value is relatively small and can be categorized as close to zero. In addition, the crystal size of the $Fe_{2.75}Mn_{0.25}O_4$/Ag filler based on XRD data also shows very small values and can be categorized as being in a single domain. Thus, the characteristics of this data represent that the SA-

$Fe_{2.75}Mn_{0.25}O_4$/Ag ferrogel has superparamagnetic properties. This result is corroborated by a previous report which states that the superparamagnetic nature of the sample is characterized by its coercive field value which is close to zero [39].

SAR Characterization

The characterization of the SA-$Fe_{2.75}Mn_{0.25}O_4$/Ag ferrogel thermal changes to the time changes using the 483 and 553 Hz frequencies. Thermal change recording is carried out every minute for a duration of 15 min. The thermal changes of SA-$Fe_{2.75}Mn_{0.25}O_4$/Ag ferrogel in every minute are presented in Figure 4. The thermal changes of the sample with a frequency of 553 Hz showed better results compared to the frequency of 483 Hz. The greater the resulting frequency, the greater the field strength applied to the sample. Increasing the field strength will have an impact on increasing the spin magnetic filler interaction $Fe_{2.75}Mn_{0.25}O_4$/Ag and in the end will contribute significantly to the increase in sample thermal.

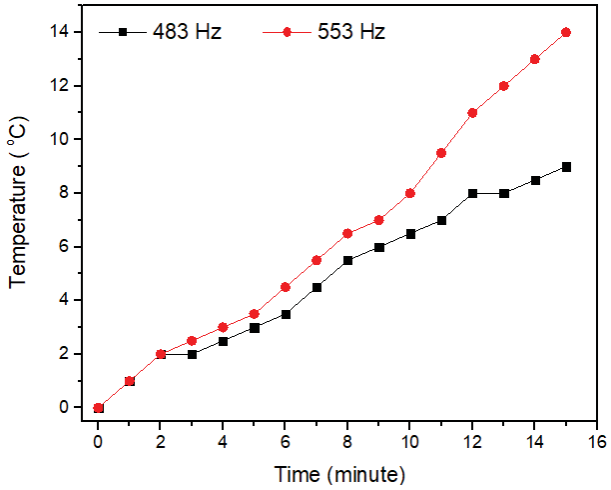

FIGURE 4. Profile of the relationship between thermal change and time changes of SA-$Fe_{2.75}Mn_{0.25}O_4$/Ag

The linear gradient of the relationship between thermal change and time change can be analyzed as a sample SAR value. The SAR value of the sample can be calculated using Equation 2 [7,40,41].

$$SAR = \left(\frac{\Delta T}{\Delta t}\right)\frac{C}{m} \tag{2}$$

t is the measurement time interval, *T* is the temperature of the sample, and *m* is the mass of the sample. While *C* is the constant of the heat capacity of the sample material obtained through Equation 3 [3].

$$C = \frac{(m_{Fe_{2.75}Mn_{0.25}O_4} \times c_{Fe_{2.75}Mn_{0.25}O_4}) + (m_{Ag} \times c_{Ag}) + (m_{SA} \times c_{SA}) + (m_{water} \times c_{water})}{m_{total}} \tag{3}$$

$c_{Fe_{2.75}Mn_{0.25}O_4}$, c_{Ag}, c_{SA}, and c_{water} are the specific heat capacities of $Fe_{2.75}Mn_{0.25}O_4$, Ag, SA and water, respectively. Whereas $m_{Fe_{2.75}Mn_{0.25}O_4}$, m_{Ag}, m_{SA}, and m_{water} are the masses of $Fe_{2.75}Mn_{0.25}O_4$, Ag, SA and water, respectively. Based on Equations (2) and (3), the SAR values of $Fe_{2.75}Mn_{0.25}O_4$/Ag ferrogel for the frequencies of 483 and 553 Hz are 0.12 and 0.24 W/g, respectively. In line with the magnitude of the frequency and the resulting thermal changes, the SAR value of $Fe_{2.75}Mn_{0.25}O_4$/Ag ferrogel with a frequency of 553 Hz is greater than that of 483 Hz. This SAR value is also better than the results of the previous report which showed a value of 0.19 W/g [21]. Thus, SA polymer was effective enough to increase the SAR value of $Fe_{2.75}Mn_{0.25}O_4$/Ag ferrogel. The presence of SA polymer increases the formation of magnetic clusters which have an impact on increasing the magnetic interaction between the nanoparticles and the nanoparticle clusters so that it has a significant effect on increasing thermal changes. However, the SAR value of $Fe_{2.75}Mn_{0.25}O_4$/Ag ferrogel is relatively smaller than the SAR value reported by Matteo Volio *et al*. which is 25 - 67 W/g [19] and Jadhav *et al*. which reported ~ 21 to ~ 81 W/g [20]. This significant difference is due to the difference in the frequency used in the magnetic induction process. Previous research reports have succeeded in detecting thermal changes

at frequencies above 100 kHz whereas in this research only used frequencies below 1 kHz. However, the increase in the SAR value of $Fe_{2.75}Mn_{0.25}O_4$/Ag ferrogel by increasing the frequency of the magnetic induction process is a positive thing for $Fe_{2.75}Mn_{0.25}O_4$/Ag ferrogel to be a potential candidate as a hypertemic agent.

SUMMARY

The SA-$Fe_{2.75}Mn_{0.25}O_4$/Ag ferrogel was successfully fabricated using the encapsulation method. Ferrogel characterization was carried out using XRD, FTIR, VSM instruments and a series of magnetic induction devices. XRD data analysis showed that the crystal sizes of $Fe_{2.75}Mn_{0.25}O_4$ and Ag nanoparticles were under 10 nm respectively. Furthermore, the results of the VSM data refinement show that the value of remanent magnetization, coercivity field and saturation magnetization of SA-$Fe_{2.75}Mn_{0.25}O_4$/Ag ferrogel are 0.094 emu/g, 0.023 T, and 8.19 emu/g, respectively. Through the crystal size of the $Fe_{2.75}Mn_{0.25}O_4$/Ag nanocomposite filler and the field coercivity field, the SA-$Fe_{2.75}Mn_{0.25}O_4$/Ag ferrogel was categorized as superparamagnetic. Meanwhile, the SAR value of SA-$Fe_{2.75}Mn_{0.25}O_4$/Ag ferrogel increased from 0.12 to 0.24 W/g with increasing magnetic induction frequency from 483 to 553 Hz. This shows that the SA- $Fe_{2.75}Mn_{0.25}O_4$/Ag ferrogel has the potential to be a material that can be applied in hyperthermia therapy.

ACKNOWLEDGMENTS

This research has been successfully conducted by financial research support from Applied Research of DRPM 2020 with contract number 10.3.50/UN32.14.1/LT/2020. The authors would like to thank DRPM for funding this research on behalf of SN.

REFERENCES

1. A. Attaran, J. Brummund, and T. Wallmersperger, Journal of Magnetism and Magnetic Materials (2016).
2. A. Shankar, A.P. Safronov, E.A. Mikhnevich, and I. V. Beketov, Journal of Magnetism and Magnetic Materials (2016).
3. L. Kubisz, A. Skumiel, E. Pankowski, and D. Hojan-Jezierska, Journal of Non-Crystalline Solids 357, 767 (2011).
4. B. Gaihre and A.C. Jayasuriya, Materials Science and Engineering: C 69, 733 (2016).
5. S. Laurent, S. Dutz, U.O. Häfeli, and M. Mahmoudi, Advances in Colloid and Interface Science 166, 8 (2011).
6. R. V Ramanujan and L.L. Lao, Magnetic particles for hyperthermia treatment of cancer. In Proc. First Intl. Bioengg. Conf 69, 1 (2004).
7. K. Murase, J. Oonoki, H. Takata, R. Song, A. Angraini, P. Ausanai, and T. Matsushita, Radiological Physics and Technology 4, 194 (2011).
8. Deng, L., Ren, J., Li, J., Leng, J., Qu, Y., Lin, C., & Shi, D. Nanoscale, 7(21), 9655-9663 (2015).
9. Sunaryono, M.N. Kholifah, Yudyanto, A. Taufiq, N. Mufti, R. Wulandari, Munasir, and M. Diantoro, IOP Conference Series: Materials Science and Engineering 367, (2018).
10. J. Rivera and D. La Rosa, Carbohydrate Polymers 200, 289 (2018).
11. E. Şalva and J. Akbuğa, Marmara Pharmaceutical Journal 21, 223 (2016).
12. G. Liu, S. Li, H. Yuan, M. Hao, Z. Yun, J. Zhao, Y. Ma, and Y. Dai, Theriogenology 113, 78 (2018).
13. J. Jin, Z. Ji, M. Xu, C. Liu, X. Ye, W. Zhang, S. Li, D. Wang, W. Zhang, J. Chen, F. Ye, and Z. Lv, ACS Biomaterials Science & Engineering 4, 2541 (2018).
14. S. Wang, Q. Ma, R. Wang, Q. Zhu, L. Yang, and Z. Zhang, Ecotoxicology and Environmental Safety 202, 110935 (2020).
15. J. Li, J. Zhao, Y. Chen, Y. Zheng, L. Zhou, J. Zhao, Y. Liu, X. Liu, and S. Wang, Science China Technological Sciences 63, 2403 (2020).
16. Kennedy, S., Roco, C., Déléris, A., Spoerri, P., Cezar, C., Weaver, J., ... & Mooney, D. Biomaterials, 161, 179-189. (2018).
17. J. Li, J. Zhao, Y. Chen, Y. Zheng, L. Zhou, J. Zhao, Y. Liu, X. Liu, and S. Wang, Science China Technological Sciences 63, 2403 (2020).
18. 18. M. Coïsson, G. Barrera, F. Celegato, L. Martino, S. N. Kane, S. Raghuvanshi, F. Vinai, P. Tiberto, Biochimica et Biophysica Acta 5, (2016).

19. M. Avolio, A. Guerrini, F. Brero, C. Innocenti, C. Sangregorio, M. Cobianchi, M. Mariani, F. Orsini, P. Arosio, and A. Lascialfari, Journal of Magnetism and Magnetic Materials 471, 504 (2019).
20. S.V. Jadhav, D.S. Nikam, V.M. Khot, S.S. Mali, C.K. Hong, and S.H. Pawar, Materials Characterization 102, 209 (2015).
21. Chusna, N. M., Hidayat, S., Hidayat, N., Mufti, N., & Taufiq, A. In IOP Conference Series: Earth and Environmental Science (Vol. 276, No. 1, p. 012062) (2019).
22. 22. Sunaryono, N. M. Chusna, N. Mufti, Munasir, J. Rajagukguk, A. Taufiq, AIP Conference Proceedings 2251, 040001 (2020).
23. A.I. Journal, M. Alomari, B.R. Jermy, V. Ravinayagam, S. Akhtar, S.A. Almofty, S. Rehman, H. Bahmdan, S. Abdulazeez, and J.F. Borgio, Artificial Cells, Nanomedicine, and Biotechnology 47, 3079 (2019).
24. A. Aarthi, M. Umadevi, R. Parimaladevi, and G. V Sathe, Journal of Molecular Liquids (2017).
25. Q. Ali, W. Ahmed, S. Lal, and T. Sen, Materials Today: Proceedings 4, 57 (2017).
26. E. Liu, M. Zhang, H. Cui, J. Gong, Y. Huang, J. Wang, Y. Cui, W. Dong, L. Sun, H. He, and V.C. Yang, Acta Pharmaceutica Sinica B (2018).
27. X. Zhao, G. Wang, and M. Hong, Materials Chemistry and Physics (2018).
28. A.S. Vorokh, Nanosystems: Physics, Chemistry, Mathematics, 9 (3), 364 (2018).
29. L.M. Tung, N.X. Cong, L.T. Huy, N.T. Lan, V.N. Phan, N.Q. Hoa, L.K. Vinh, N.V. Thinh, L.T. Tai, D.-T. Ngo, K. Mølhave, T.Q. Huy, and A.-T. Le, Journal of Nanoscience and Nanotechnology 16, 5902 (2016).
30. C. C., X. D.-L., G. L.-Y., C. Y.-P., L. X.-D., W. Y.-F., Z. D., W. Y.-Y., Z. Y.-X., H. H., and G. H.-Y., Journal of Biomedical Materials Research - Part B Applied Biomaterials 106, 2029 (2018).
31. S. Venkateswarlu, B. Natesh Kumar, B. Prathima, K. Anitha, and N.V. V Jyothi, Physica B: Condensed Matter 457, 30 (2015).
32. Z. Hassannejad and M.E. Khosroshahi, Optical Materials 35, 644 (2013).
33. Y.T. Prabhu, K.V. Rao, B.S. Kumari, V.S.S. Kumar, and T. Pavani, International Nano Letters 5, 85 (2015).
34. E. Tahmasebi and Y. Yamini, Analytica Chimica Acta 756, 13 (2012).
35. A. Taufiq, E.G. Rachman Putra, A. Okazawa, I. Watanabe, N. Kojima, and S. Pratapa, Journal of Superconductivity and Novel Magnetism 28, 2855 (2015).
36. W. Shao, H. Liu, X. Liu, S. Wang, J. Wu, R. Zhang, and H. Min, Carbohydrate Polymers 132, 351 (2015).
37. S.R. Derkach, N.G. Voron, N.I. Sokolan, D.S. Kolotova, Y.A. Kuchina, S.R. Derkach, N.G. Voron, N.I. Sokolan, and D.S. Kolotova, Journal of Dispersion Science and Technology 0, 1 (2019).
38. Y. Han and L. Wang, Journal of the Science of Food and Agriculture 97 (4), 1295-1301 (2017).
39. A.M. Escamilla-pérez, D.A. Cortés-hernández, J.M. Almanza-robles, and D. Mantovani, Journal of Magnetism and Magnetic Materials 374, 474 (2015).
40. Mehdaoui, B., Meffre, A., Carrey, J., Lachaize, S., Lacroix, L. M., Gougeon, M., ... & Respaud, M. Advanced Functional Materials, 21(23), 4573-4581 (2011).
41. Huang, S., Wang, S. Y., Gupta, A., Borca-Tasciuc, D. A., & Salon, S. J. Measurement Science and Technology, 23(3), 035701 (2012).
42. Lao, L. L., & Ramanujan, R. V. Journal of materials science: Materials in medicine, 15(10), 1061-1064 (2004).